Proceedings of the 7th WSEAS International Conference on Neural Networks, Cavtat, Croatia, June 12-14, 2006 (pp67-72)

Raising of Indecision of a Phase-Shift Laser Rangefinder thanks to feedforward MLP Neural Network

L.GATET, H. TAP-BETEILLE, M. LESCURE
Electronics laboratory LEN7
INPT - ENSEEIHT
2 Rue C. Camichel, BP 7122, 31071 Toulouse Cedex 7
FRANCE

Abstract : A feasibility study has been achieved concerning the raising of indecision on a distance value measured by a phase-shift laser rangefinder, by implementing a Neural Network in the optical head. The NN role is to give an approximation of the distance to measure, using the output signal amplitude of the rangefinder, in order to remove the indecision modulo 2π due to the phase shift measurement. Thus, the neural network has to be able to achieve the function "$1/D^{1/2}$" in order to invert the "$1/D^2$" law relative to the evolution of the photoelectric output signal amplitude of the rangefinder according to the distance D. Thanks to this system, it is possible to obtain a very high resolution on the distance measurement for a range three times wider than the one limited by the $2k\pi$ indecision. Behavioural computer simulations of the system has shown very satisfying results. That is the reason why an analog implementation of the neural network is currently achieved.

Key-Words: neural network, multi-layer perceptron, backpropagation algorithm, distance measurement, heterodyne laser rangefinder, analog implementation.

1 Introduction

Main application domains of neural network (NN) [1-2] are classification and detection [3-4] and approximation of non-linear functions in order to model or to linearise some physical phenomenon [5]. Among the different kinds of NN, Multi-Layers Perceptrons (MLP) networks have the advantage to be simple and to be able to linearise continuously some functions. MLP application domains are very wide, from the help for the handwritten character recognition [6-7] to the linearisation of non-linear data transfer of high-power amplifiers for satellites telecommunications [5,8], or pattern detection [9].

In order to achieve real-time distance measurement thanks to a phase-shift laser rangefinder, data processing has to be fast and continuous. Furthermore, the system has to be trained in various simulation conditions, such as defocalisation, temperature changes or crosstalk, in order to avoid bad data processing. That is the reason why it has been chosen to design a MLP-type NN, with analog circuits for speed, chip size and consumption reasons. Indeed, analog neural network (ANN) allows faster data processing because signals are analog from the rangefinder output up to the NN output. Thus, all bandwidth limitation due to analog-to-digital converters is prevented. Moreover, obtaining the same precision with a digital NN with regards to an analog one would require a high number of bits and transistors for achieving exactly the same operations, especially for sigmoid functions. Thus, analog implementation leads to interesting space and consumption gain.

The complete system is presented in part 2. The calibration phase and the design of the neural network are presented in part 3.

2 System description

2.1 Phase-Shift Laser Rangefinder with heterodyne mixing

Laser ranging is an optoelectronic way used for achieving distance measurement [10-12]. Distance value can be deduced from the time-of-flight measurement. Time-of-flight methods can be divided into three categories: pulsed technique [13], Frequency Modulation Continuous Wave (FMCW) method [14-16], and phase-shifting measurement [17]. The last studies achieved in the laboratory has shown that the phase-shift laser rangefinder is very promising [18]. That is the reason why the improvement of the method by increasing easily the measurement range is interesting.

The phase-shift laser rangefinder principle is given in Fig.1. A c.w. sinusoidal modulation of the light power emitted by the laser diode is used, with a constant frequency f_{RF}. The phase-shift $\Delta\varphi$ existing between the emitted wave and the received one is measured. This phase-shift $\Delta\varphi$ is linked to the time of flight following the relationship:

$$\Delta\varphi = 2\pi f_{RF}\tau_D \quad (1)$$

where $\tau_D = \frac{2D}{c}$ is the time of flight, with D the distance to measure and c the celerity of light in

vacuum ($c = 3.10^8$ m/s). As distance is determined from a phase-shift, and as phase-shift is measured modulo 2π, distance value is given with a "$2k\pi$-indecision". Thus, the maximum measurement range Λ without indecision is:

$$\Lambda = \frac{c}{2f_{RF}} \quad (2)$$

Indeed, the f_{RF} frequency must be high so that the resolution of the measurement is good. The distance resolution δD is given by:

$$\delta D = \frac{1}{2\pi f_{RF}} \frac{c}{2} \delta\varphi \quad (3)$$

Thus, the higher the frequency f_{RF} is, the better the sensitivity $S_D = \frac{\delta D}{\delta\varphi}$ is, but the smaller the measurement range is. In our case, we choose f_{RF} = 166MHz; that leads to a very good resolution δD of 50µm on the distance measurement, considering a reasonable resolution on the phase measurement of $\delta\varphi = 0.02°$, but for a measurement range Λ of only 0.9m. As realising a phase-shift measurement is not easy at high frequencies, a heterodyne technique is used, which allows to make phase measurement at an intermediate frequency $f_{IF} = |f_{RF} - f_{LO}|$ (Fig.1). We consider that the frequency mixing keeps the same phase-shift. The photoelectric signal received by the avalanche photodiode (APD) at frequency $f_{RF}(\Delta\varphi)$ is mixed with a reference signal which is supplied from a local oscillator and whose frequency is f_{LO}. The output signal of the mixer is the sum of two signals, whose respective frequencies are $f_{RF}(\Delta\varphi)+f_{LO} = f_{HF}(\Delta\varphi)$ and $f_{RF}(\Delta\varphi)-f_{LO} = f_{IF}(\Delta\varphi)$ the intermediate frequency. In order to delete high frequency $f_{HF}(\varphi)$ and to obtain the best signal to noise ratio, a band-pass filter tuned on $f_{IF}(\Delta\varphi)$ is used. For measuring the phase-shift $\Delta\varphi$, the f_{IF} output signal of the band-pass filter is compared with a reference signal at the frequency f_{IF}. This reference signal is provided by the output of another band-pass filter centred on f_{IF} that received at its input the mixing of both signals coming from the RF and LO oscillators (Fig.1).

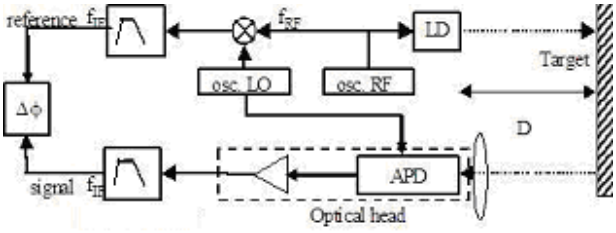

Fig.1: Block diagram of the phase shift laser range finder using a heterodyne technique. Pass band filters tuned to the intermediate frequency enhance the signal-to-noise ratio of the photoelectric signal. A transimpedance amplifier is placed at the output of the APD.

2.2 Determination of the function g that has to be approximated by the ANN

Our objective is to use the amplitude of the a.c. photoelectric signal after the pass-band filter and the approximation properties of neural networks for raising the indecision on the distance measurement and thus being able to increase the distance measurement range from 1m to 4m with the same resolution. For that, the neural network has to achieve a function so that its output is a voltage proportional to the distance:

$$VoutNN = K_0 D \quad (4)$$

Let us call g the function achieved by the NN.

$$VoutNN = g(VinNN) . \quad (5)$$

From a structural point of view, the NN must have one single input (relative to the signal amplitude VinNN at the output of the band pass filter) and one single output (whose voltage VoutNN has to be proportional to the distance to measure). For the number of neurons placed on the hidden layer, the discussion will be developed subsequently.

As the illuminated zone is considered to be smaller than the non-cooperative target surface and the source is supposed lambertian, the a.c. output photoelectric current of the APD has an amplitude that varies according to the inverse of the square distance D [19]. The photoelectric signal amplitude at the transimpedance output follows:

$$VoutTRANS = Z_t i_{APD} = f(D) = K_1 \frac{\cos(\theta_0)}{D^2} \quad (6)$$

with Z_t the transfer function of the transimpedance amplifier, θ_0 the laser beam incidence angle according to the perpendicular to the target surface, and K_1 a proportionality coefficient relative to the emitter, the optical transfer, and the APD response.

$$K_1 = T_\lambda T_R S_\lambda M Z_t \frac{\rho}{\pi} P_{LD} A_R \quad (7)$$

where T_λ is the emitter transmission coefficient for a given laser wavelength, T_R the receiver transmission coefficient of the optics, S_λ the APD spectral response of the primary photocurrent, M the photoelectric gain of the APD, ρ the diffusing reflection coefficient of a non-cooperative target, P_{LD} the modulated power of the transmitted laser beam and A_R the surface of the APD.

For a painted wall as target, theoretical and measured curves relative to the photoelectric signal amplitude between 0.5m and 3.5m are shown in Fig.2.

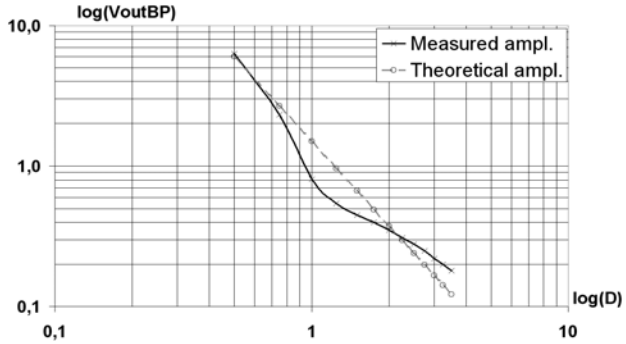

Fig.2: Representation in log-log scale of the output voltage amplitude of the APD as a function of the distance. The ideal characteristic curve is dashed; the measurement points are joined by the solid curve.

The photoelectric signal amplitude VoutBP observed at the band-pass filter output is proportional to the transimpedance output amplitude VoutTRANS. As both curves are close, (6) is verified. Thus, as the neural network input VinNN receives a signal relative to the pass-band filter output amplitude VoutBP, the function g to be achieved by the neural network in order to obtain VoutNN as a linear function according to the distance D is :

$$g(\text{VinNN}) = g(\text{VoutBP}) = \text{VoutNN} = \frac{K_2}{\sqrt{\text{VinNN}}}$$

$$= \frac{K_2}{\sqrt{\frac{K_1 \cos(\theta_0)}{D^2}}} = K_0 D \qquad (8)$$

The complete system is shown in Fig.3.

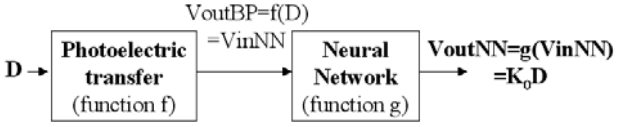

Fig.3: Function g that has to be achieved by the ANN in order to obtain an output voltage linear with respect to the distance (θ is considered to be constant).

In order to simplify the system, and with the idea to use a feedforward neural network (static, without feedback on the weights), the a.c. signal is converted into a d.c. voltage proportional to the r.m.s. of the IF photoelectric signal (Fig.4). This d.c. voltage is then injected into the neural network.

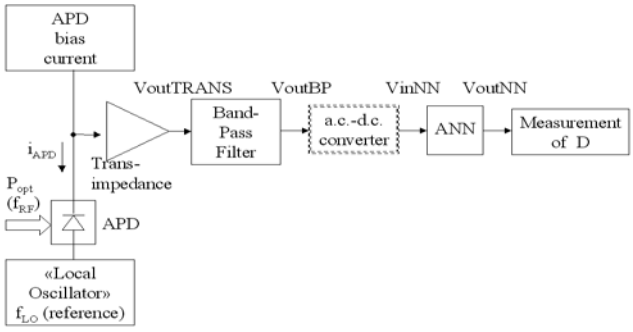

Fig.4: Conversion of the alternative voltage at the output of the band-pass filter.

3 Achievement of the ANN for a linear distance measurement

3.1 Structure

For summarising, the structure of the NN to achieve is a feedforward single-input single-output MLP-type NN. The number of neurons in the hidden layer is fixed at 3 (Fig.5). This number is sufficient for having a good approximation without having a too complex structure. When simulations are done with more neurons, the precision of simulation results is a little bit better, for a calculation time a little bit longer, but for a structure more complex. For two neurons on the hidden layer, the algorithm cannot converge. Every weight and bias value has been determined by Matlab simulations in order to calibrate the ANN.

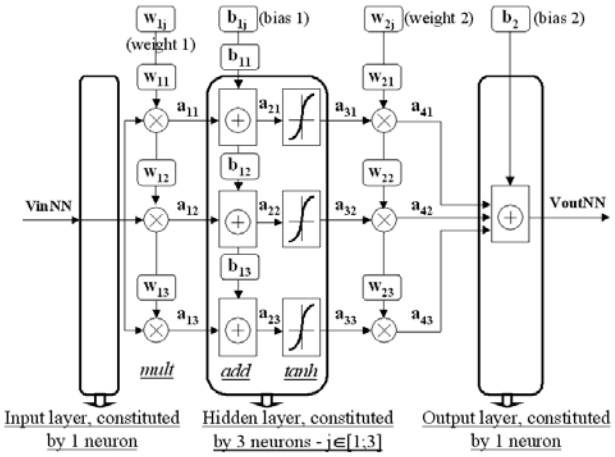

Fig.5: Structure of the ANN developed: It is constituted by three layers, with one neuron in the input layer, one in the output layer and three in the hidden layer.

3.2 Determination of weight and bias values - Calibration phase

To calculate weights and biases, the method described in Fig.6 is used.

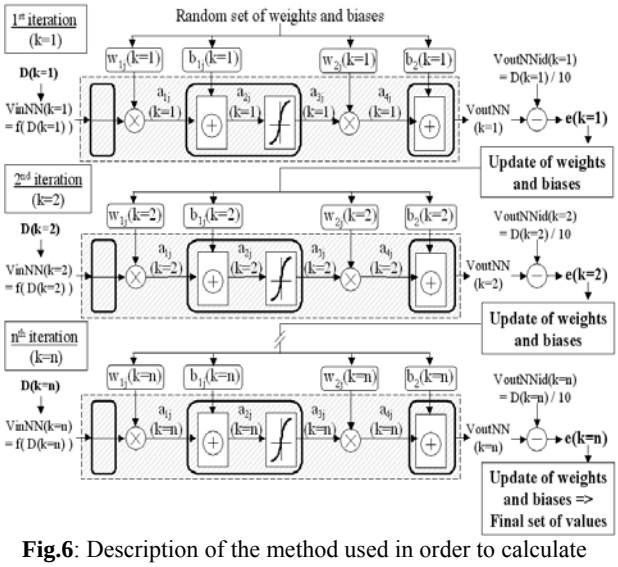

Fig.6: Description of the method used in order to calculate weights and biases.

First, in order to train the ANN, a set of random NN input values is determined. VinNN(k) is the NN input voltage at iteration k, corresponding to a certain kind of target with a certain incidence angle for a random distance D(k) from a defined number of distances between 1m and 4m.

Then the different equations that take place into the ANN are described. Each intermediate output of the ANN is called a_i (Fig.5). Each a_i is a vector of three values a_{ij} (with $j \in [1;3]$), relative to the fact that there are three neurons present in the hidden layer. Weights w1(k,:) (respectively biases b1(k,:) and weights w2(k,:)) corresponds to the three values w_{1j} (respectively b_{1j} and w_{2j}) at the iteration k. b2(k) is the bias value b2 at iteration k.

```
a1=Ka1*VinNN(k)*w1(k,:); % Output of the
multipliers between input neuron and hidden layer
a2=a1+Ka2*b1(k,:);          % Output of the hidden
layer adders
a3=Ka3*tanh(Kth*a2);    % Output of the
hyperbolic tangents of the hidden layer
a4=Ka4*a3*w2(k,:);      % Output of the
multipliers between hidden layer and output neuron
VoutNN(k)=sum(a4)+b2(k);    % Output of the last
adder / ANN output
```

Thus, for every Ka_i and K_{th} taken equal to 1,

$$VoutNN(k)=b_2(k)+\sum_{i=1}^{3} w_{2i}(k).\tanh(w_{1i}(k).VinNN(k)+b_{1i}(k)). \quad (9)$$

Then the iterative part is described, which allows to update weights and biases at each iteration, so that they converge to a definitive value. If we look at Fig.6, at the end of the first iteration, NN output VoutNN(k=1) is compared to the ideal output value VoutNNid(k=1). This comparison leads to a difference e(k=1) between both values, that is used to calculate the new weight and bias values with the help of an algorithm called error backpropagation algorithm. The algorithm type used is the gradient algorithm. The weights and biases update is done by subtracting a present value of weight or bias to the error gradient corresponding to the considered weight or bias ((10) to (14)).

$$b_2(k+1)=b_2(k)+\mu\_b_2.\,\mathrm{grad}_{b2}(e(k)) = b_2(k)+\mu\_b_2.\frac{\partial e(k)}{\partial b_2} \quad (10)$$

$$w_2(k+1)=w_2(k)+\mu\_w_2.\,\mathrm{grad}_{w2}(e(k)) = w_2(k)+\mu\_w_2.\frac{\partial e(k)}{\partial w_2} \quad (11)$$

$$b_1(k+1)=b_1(k)+\mu\_b_1.\,\mathrm{grad}_{b1}(e(k)) = b_1(k)+\mu\_b_1.\frac{\partial e(k)}{\partial b_1} \quad (12)$$

$$w_1(k+1)=w_1(k)+\mu\_w_1.\,\mathrm{grad}_{w1}(e(k)) = w_1(k)+\mu\_w_1.\frac{\partial e(k)}{\partial w_1} \quad (13)$$

with e(k)=VoutNNid(k) - VoutNN(k)
and VoutNN(k) =

$$[b_2(k)+\sum_{j=1}^{3} w_{2j}(k).\tanh(w_{1j}(k).VinNN(k)+b_{1j}(k))] \quad (14)$$

μ_w_1, μ_b_1, μ_w_2 and μ_b_2 are called convergence speed, associated to each weight and bias. Once the update is done, the second iteration begins, with a new input value and a new ideal associated output value (Fig.6 – 2nd iteration).

Iterations stop as soon as the function achieved by the NN is considered to be close enough to the ideal output, in the desired input interval. For that, the Signal-to-Error-Ratio (SER) is calculated with the help of a chosen number of the last output values VoutNN(k) and associated error e(k). SER allows to quantify the aptitude of the NN to approximate the desired function (15).

$$SER=10.\log_{10}\left(\frac{\sum_{k=npts-nptsSER}^{npts} VoutNN(k)}{\sum_{k=npts-nptsSER}^{npts} e(k)}\right) \quad (15)$$

with npts the algorithm iterations number and nptsSER the number of values chosen at the end of the algorithm to calculate the SER. Precision is determined by the user through SER value. Higher the SER is, better the function to approximate is fitted. When SER has reached the desired value, iterations stop, and weight and bias values are set (Fig.6 – end of the nth iteration).

Fig.7 shows an example of convergence of the algorithm. 250000 iterations were achieved for obtaining a SER equal to 40dB. The 5000 last iterations have been plotted in Fig.7. Fig.7-a to 7-d show that the weights and biases have converged to a definitive value. Fig.7-f shows the input voltage values relative to the different random distances from 0.5m to 4m represented in Fig.7-e. The solid curve of Fig.7-g represents the ANN output for the different input voltage values plotted in Fig.7-f, with the weights and biases set plotted in Fig.7-a to 7-d. This curve can hardly been distinguished from the dashed ideal curve VoutNNid, that is a linear representation of Fig.7-e relative to the different distance values (VoutNNid = D/10). Thus the ANN achieves quite perfectly the function g with the set of weight and bias values represented in Fig.7-a to 7-d. Fig.7-h shows that the absolute value of the error is less than 5mV for the 50 last iterations. Thus, the network calibrated with the set of weight and bias values represented in Fig.7-a to 7-d is able to achieve function g in order to obtain an ANN output voltage proportional to the distance.

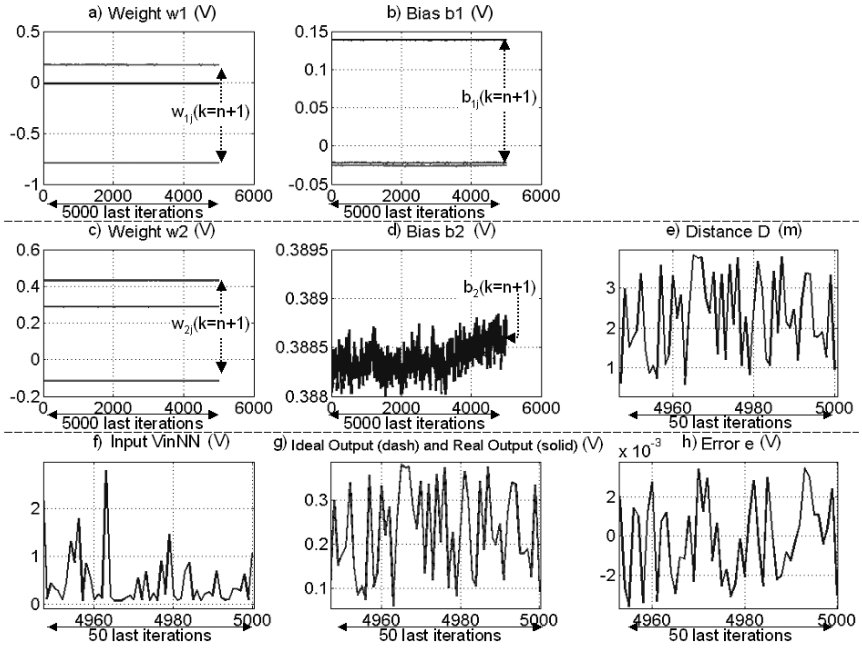

Fig.7: From a) to d) : Weights and biases variation during the 5000 last iterations; e) Random distance values between target and rangefinder; f) The corresponding input DC value VinNN; g) ANN output voltage VoutNN with the weights and biases set represented in a) to d) (solid) and the ideal output (dash). There is to note that both are superimposed; h) Error between both curves represented in g)

The ANN test is represented in Fig.8, with the final values of weights and biases found in Fig.7-a to 7-d, for distance values that vary linearly from 0.5m to 4m. ANN output plotted in Fig.8-b is almost linear with respect to the distance. The absolute value of the error between ideal and real ANN output curves shown in Fig.8-c is less than 6mV on the whole distance range. The relative error shown in Fig.8-d is less than 5% between 0.6m and 4m. That is sufficient to have a good distance approximation and to raise the $2k\pi$ indecision of the phase-shift rangefinder. Thus these simulations with Matlab software justify the fact that it is possible to achieve a precise distance measurement for a distance range three times wider thanks to the NN.

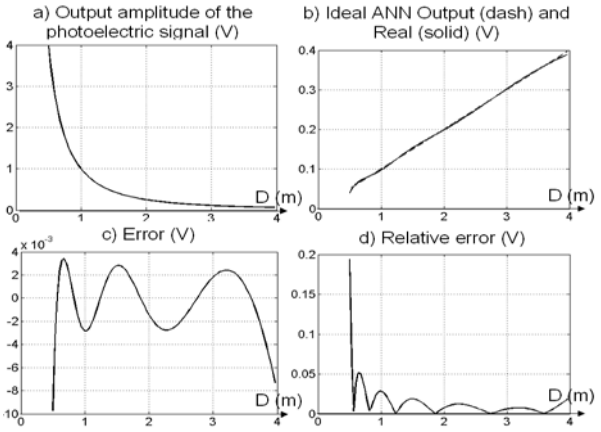

Fig.8: a) Input voltage variation VinNN according to the distance, from 0.5m to 4m;
b) ANN output voltage with the final weights and biases determined at the last iteration of the algorithm (solid) and the ideal output (dash);
c) Error between both previous curves;
d) Relative error.

3.3 Conception of the circuit with PSpice software

Once the network has been trained with Matlab and that the final set of weight and bias values is fixed, so that we can obtain a good approximation of the function, electronic simulations are achieved with PSpice. First, behavioural simulations are performed, using ideal multiplier, adder and hyperbolic tangent cells. Each weight or bias value found with Matlab is injected in its corresponding cell. These behavioural electronic simulations give identical results compared to the ones found with Matlab (Fig.9).

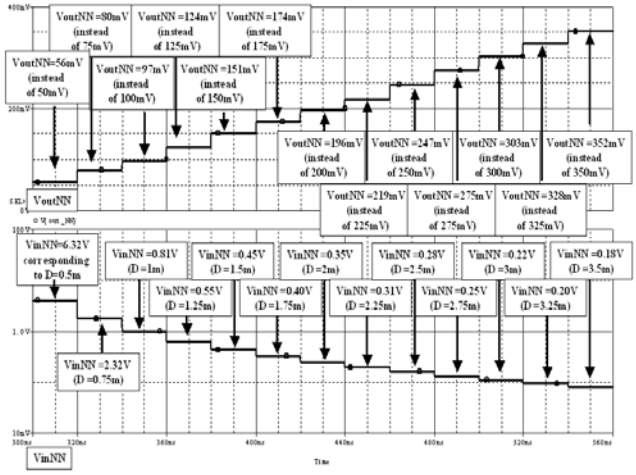

Fig.9: Example of simulation results. Ideal Output: VoutNN=D/10. Error is less than 6mV.

Thus, hardware integration of the ANN will allow to improve the distance measurement range by a factor approximately equal to three, with the same high resolution.

4. Conclusion and perspectives

This study is the first one achieved for the implementation of an analog neural network into a phase-shift laser rangefinder. Our objective is to easily remove the $2k\pi$ indecision on the phase measurement and thus to obtain a measurement range three times wider without using multiple modulation frequencies of the laser diode. Matlab software simulations give a SER higher than 40dB and a relative error smaller than 5% on the whole interval of distance from 0.6m to 4m. The performances obtained allow to reach a very good approximation of equation (8) and yield to an ANN output voltage proportional to the distance. As behavioural electronic simulations have confirmed the expected functioning of the network, the next step of the study is the design and the integration in an ASIC.

References

[1] J.M Bishop, R.J Mitchell, Neural networks-an introduction , *Neural Networks for Systems: Principles and Applications*, IEE Colloquium on 25 Jan 1991, pp.1/1 - 1/3

[2] Introduction to artificial neural networks , *Electronic Technology Directions to the Year 2000*, Proceedings, pp.36 – 62 (23-25 May 1995)

[3] Lim Ee Hui, K.P. Seng; K.M. Tse, RBF neural network mouth tracking for audio-visual speech recognition system, *TENCON 2004*, *2004 IEEE Region 10 Conference*, Volume A, pp.84 - 87 Vol. 1 (21-24 Nov. 2004)

[4] Fan Yang, M. Paindavoine, Implementation of an RBF neural network on embedded systems: real-time face tracking and identity verification, *Neural Networks, IEEE Transactions on Volume 14*, Issue 5, pp.1162 – 1175 (Sept. 2003)

[5] F. Castanie, D. Roviras, Neural networks in space communications, *Digital Signal Processing, 2002. DSP 2002. 2002 14th International Conference on Volume 1*, pp.3 - 7 vol.1 (2002)

[6] N. Mozayyani, A.R. Baig, G. Vaucher, A fully-neural solution for online handwritten character recognition, *Neural Networks Proceedings*, *1998. IEEE World Congress on Computational Intelligence*, Volume 1, pp.160 - 164 vol.1 (4-9 May 1998)

[7] S. Knerr, L. Personnaz, G. Dreyfus, Handwritten digit recognition by neural networks with single-layer training, *Neural Networks, IEEE Transactions*, Volume 3, Issue 6, pp.962 – 968 (Nov. 1992)

[8] F. Langlet, D. Roviras, A. Mallet, F. Castanie, Mixed analog/digital implementation of MLP NN for predistortion, *Neural Networks, 2002. IJCNN '02. Proceedings of the 2002 International Joint Conference on Volume 3*, pp.2825 – 2830 (12-17 May 2002)

[9] A.R. De Almeida, E.O. Freire, C.A. Ronnow, J.E.S. Vianna, R.M. Rosi, Neural network-based geometric references recognition applied to ultrasound echo signals, *Circuits and Systems, 2000. Proceedings of the 43rd IEEE Midwest Symposium*, Volume 3, pp.1344 - 1347 vol.3 (8-11 Aug. 2000)

[10] T. Bosch, M. Lescure, *Laser Distance measurement*, SPIE Milestone series, Vol.MS115, Washington, 1995.

[11] S. Donati, *Electro-optical instrumentation, sensing and measuring with lasers*, Prentice Hall, 2004

[12] M.C. Amann, T. Bosch, M. Lescure, R. Myllylä, M. Roux, Laser ranging: a critical review of usual techniques for distance measurement, *Optical Engineering* 40 (1) pp.1-10 (2001)

[13] H. Ailisto, V. Heikinnen, R. Mitikka, R. Myllyla, J. Kostamovaara, A. Mantyniemi, M. Koskinen, Scannerless imaging pulsed-laser range finding, *J. Opt. A: Pure Appl. Opt.* 4**,** pp.337-346 (2002)

[14] B. Journet, G.Bazin, A low-cost laser range-finder based on an FMCW-like method, *IEEE Trans. Instrum. Meas.*,49, pp.840-843 (2000).

[15] D. Dupuy, M. Lescure, H. Tap-Béteille, Analysis of an avalanche photodiode used as an optoelectronic mixer for a Frequency Modulated Continuous Wave laser range finder, *Journal of Optics A : Pure Appl. Opt.* 4, pp.332-336 (2002)

[16] D. Dupuy, M. Lescure, Improvement of the FMCW Laser Range-Finder by an APD Working as an Optoelectronic Mixer, *IEEE Transactions on Instrumentation and Measurement*, 51(5), pp.1010-1014 (2002).

[17] S. Poujouly, B. Journet, Laser range finding by phase-shift measurement: moving towards smart systems, *Proceedings of the SPIE Machine Vision and Three-Dimensional Imaging Systems for Inspection and Metrology*, Boston, MA, USA, 4189, pp.152-160, Nov. 5-8 (2000)

[18] D. Castagnet, H. Tap-Béteille, M. Lescure, APD-based heterodyne optical head of a phase-shift laser rangefinder, *Optical Engineering,* to be published

[19] T. Bosch, M. Lescure, Experimental determination of the useful reflexion coefficient of non-cooperative targets for a time-of-flight laser rangefinder, *Optical Review*, Vol.2, No.4, pp.289-291 (1995)